Electronic Supplementary Material (ESI) for Physical Chemistry Chemical Physics.

Supporting Information: Influence of the extent of hydrophobicity on water organization and dynamics on 2D graphene oxide surfaces

Rajasekaran M,[a] and K. Ganapathy Ayappa*[a,b]

1 Charge computation and electrostatic potentials

During the charge calculation for the different surfaces using Gaussian, the edge carbon atoms were terminated with hydrogen. In order to create the periodic structures for the GCMC and MD simulations, the terminal hydrogen atoms are removed, and the charge transferred to the bonded carbon atom. We also computed the electrostatic potential energy to understand the differences in the charges across the GO surface and understand the origin of asymmetry observed density profiles (see Fig. 2 in the main manuscript). These electrostatic potential energy maps are obtained by computing the electrostatic interaction energy between the GO surface and a SPC water molecule on a two-dimensional grid of $\Delta x = 0.41$ Å and $\Delta y = 0.35$ Å. The oxygen atom of a water molecule is located at the position of $z = 5.2$ Å for the surface $Z > 0$ cases, and for the $z < 0$ cases, it is located at $z =$ -5.2 Å. The water molecule is positioned on the GO surface with the HH vector of water molecule making an angle of 19.2° with surface normal. The water molecule with the initial orientation at $x = 0$ and $y = 0$ is translated across the GO surface with the grid dimensions of Δx and Δy to compute the 2D interaction energy map. Figure S1 illustrates the electrostatic potential energy map of GO surface of $H_R = 0$ for both sides $z < 0$ and $z > 0$. For the surface ($z > 0$), the lowest electrostatic energy sites are observed when compared with the surface ($z < 0$)(Fig. S1a and b). The lowest energy sites are shown in the molecular structure of GO for both sides. A difference in the electrostatic energy on the surfaces ($z > 0$ and $z < 0$) is noticed for all the GO surfaces (Figs. S2, S3, S4). This clearly explains the origins of the density asymmetry observed in the density distributions. We point out that the greatest charge asymmetry is observed for $H_R = 1$ (Fig. S3) and the extent of the asymmetry reduces for larger H_R values as the extent of the graphene regions increase (Fig. S4)

---

[a] Department of Chemical Engineering, Indian Institute of Science, Bangalore, India 560012. Fax: +91-80-2360-8121; Tel: +91-80-2293 2769; E-mail: ayappa@iisc.ac.in
[b] Centre for Biosystems Science and Engineering, Indian Institute of Science, Bangalore, India 560012

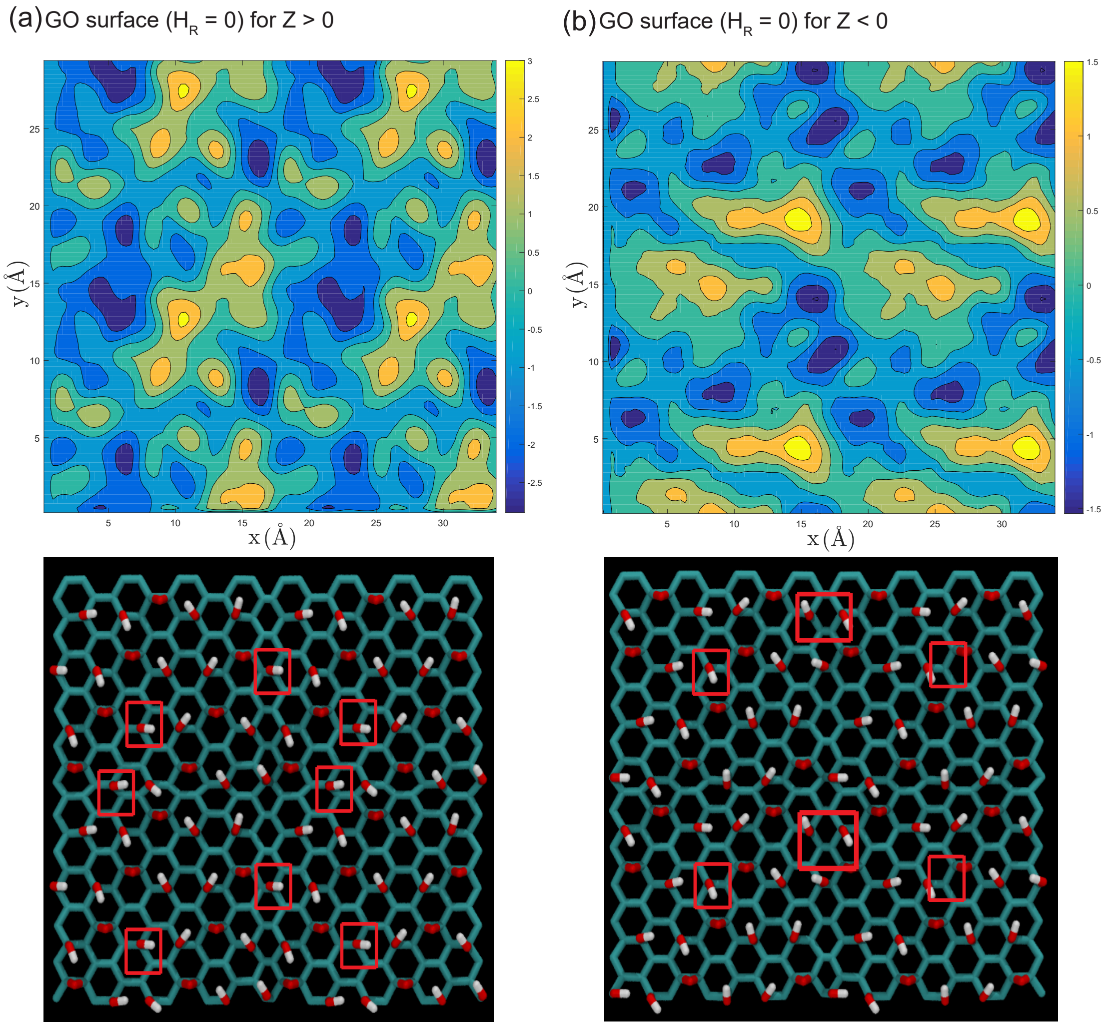

Fig. S1 (a) Electrostatic potential energy contour for GO surface of $H_R = 0$ for $z > 0$ along with molecular structure of GO surface. GO surface is shown in licorice representation and Carbon, oxygen and hydrogen atoms in the GO surface are shown in cyan, red, and white colors, respectively. (b) Electrostatic potential energy contour for GO surface of $H_R = 0$ for $z < 0$. The unit of electrostatic potential energy shown in the color map is kcal/mol. The interaction sites marked in the GO molecular structure correspond to the lowest electrostatic energy in the potential map.

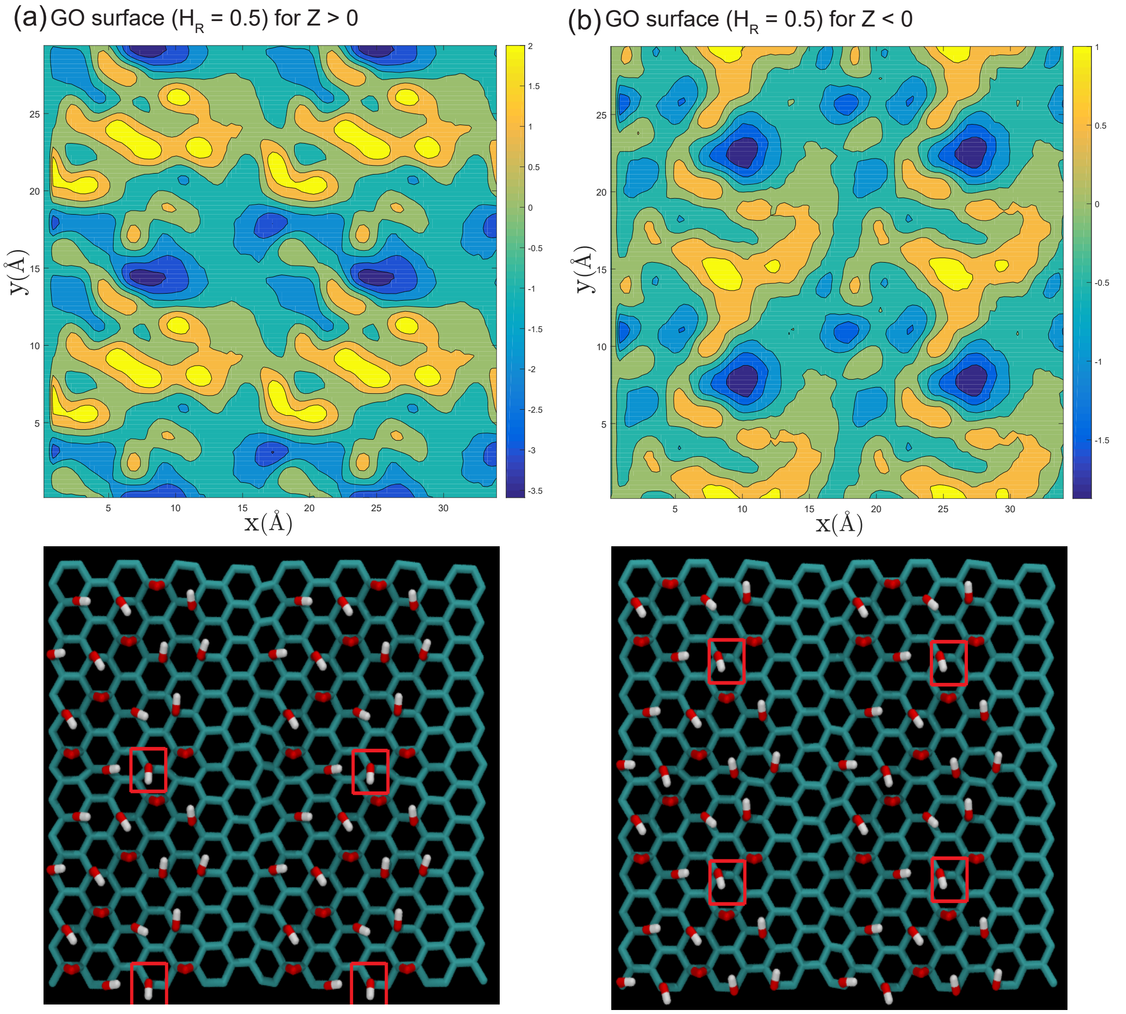

(a) GO surface (H_R = 0.5) for Z > 0

(b) GO surface (H_R = 0.5) for Z < 0

Fig. S2 (a) Electrostatic potential energy contour for GO surface of $H_R = 0.5$ for $z > 0$ along with molecular structure of GO surface, (b) Electrostatic potential energy contour for GO surface of $H_R = 0.5$ for $z < 0$. The unit of electrostatic potential energy shown in the color map is kcal/mol. The interaction sites marked in the GO molecular structure correspond to the lowest electrostatic energy in the potential map.

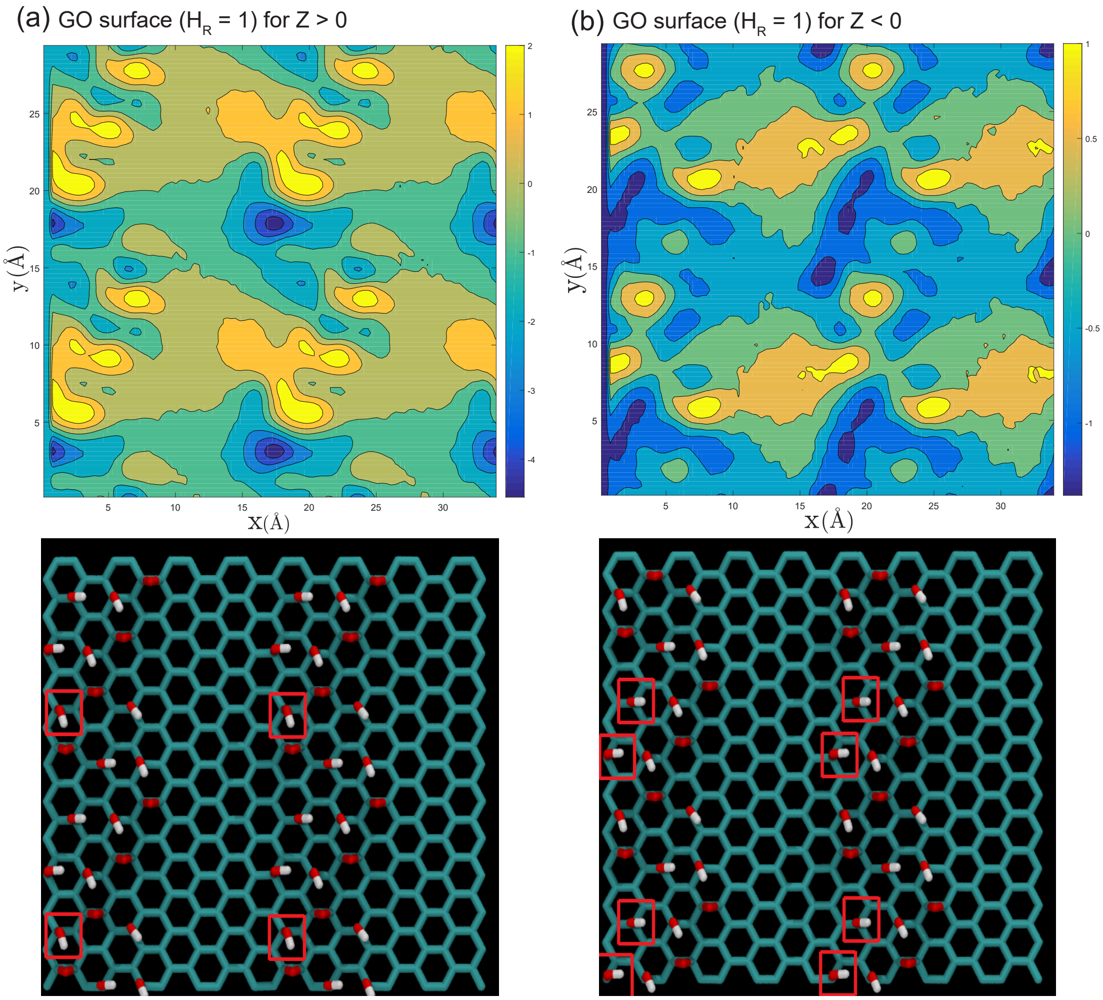

Fig. S3 (a) Electrostatic potential energy contour for GO surface of $H_R = 1$ for $z > 0$ along with molecular structure of GO surface, (b) Electrostatic potential energy contour for GO surface of $H_R = 1$ for $z < 0$. The unit of electrostatic potential energy shown in the color map is kcal/mol. The interaction sites marked in the GO molecular structure correspond to the lowest electrostatic energy in the potential map.

(a) GO surface (H_R = 2) for Z > 0

(b) GO surface (H_R = 2) for Z < 0

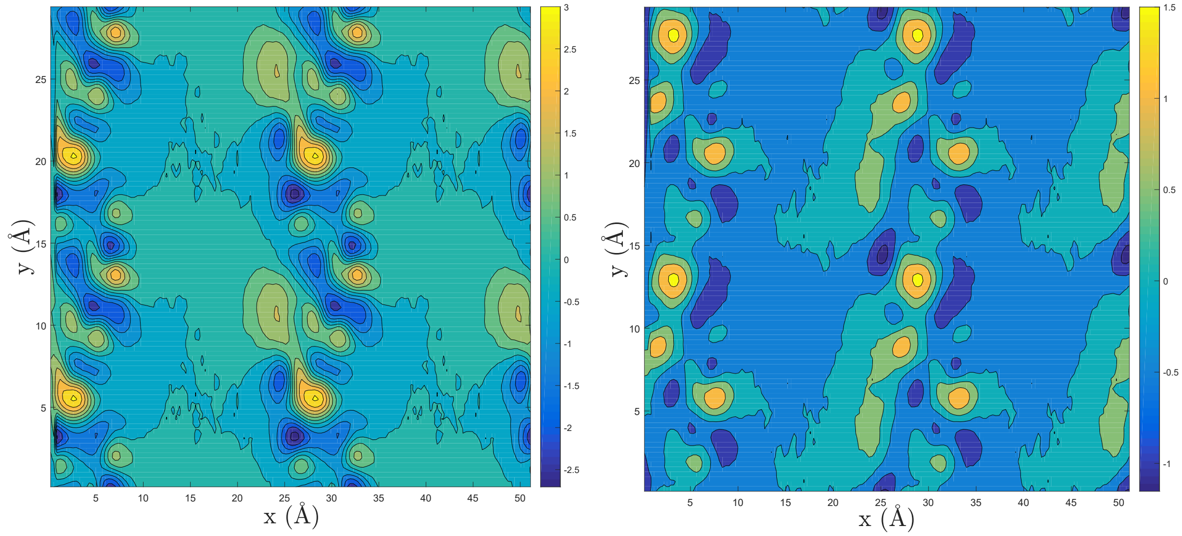

(c) GO surface (H_R = 3) for Z > 0

(d) GO surface (H_R = 3) for Z < 0

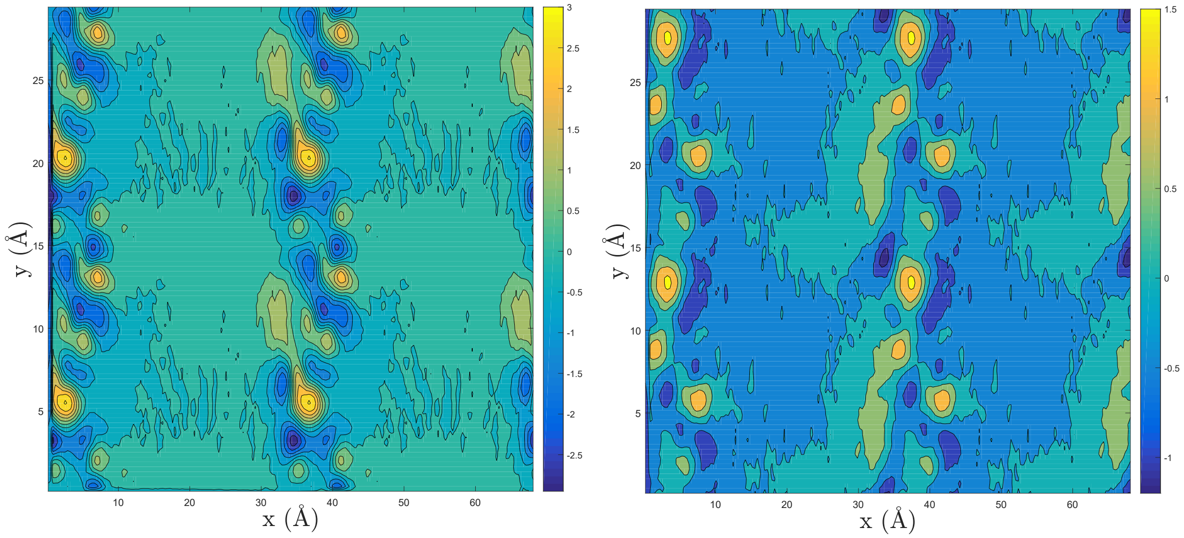

Fig. S4 (a) Electrostatic potential energy contour for GO surface of $H_R = 2$ for $z > 0$, (b) Electrostatic potential energy contour for GO surface of $H_R = 2$ for $z < 0$, (c) Electrostatic potential energy contour for GO surface of $H_R = 3$ for $z > 0$, and (d) Electrostatic potential energy contour for GO surface of $H_R = 3$ for $z < 0$.The unit of electrostatic potential energy shown in the color map is kcal/mol.

2 GCMC Simulations

The number of water molecules adsorbed on the GO surfaces of H_R = 0, 0.5, 1, 2 and 3, as a function of MC cycles for relative pressures of 0.3 to 0.9 are shown in Fig. S5 and the ensemble-averaged number of adsorbed water molecules on GO surfaces of H_R = 0, 0.5, 1, 2 and 3, are shown in Table S1. In Fig. S6, the adsorption isotherm is presented in terms of water weight ratio.

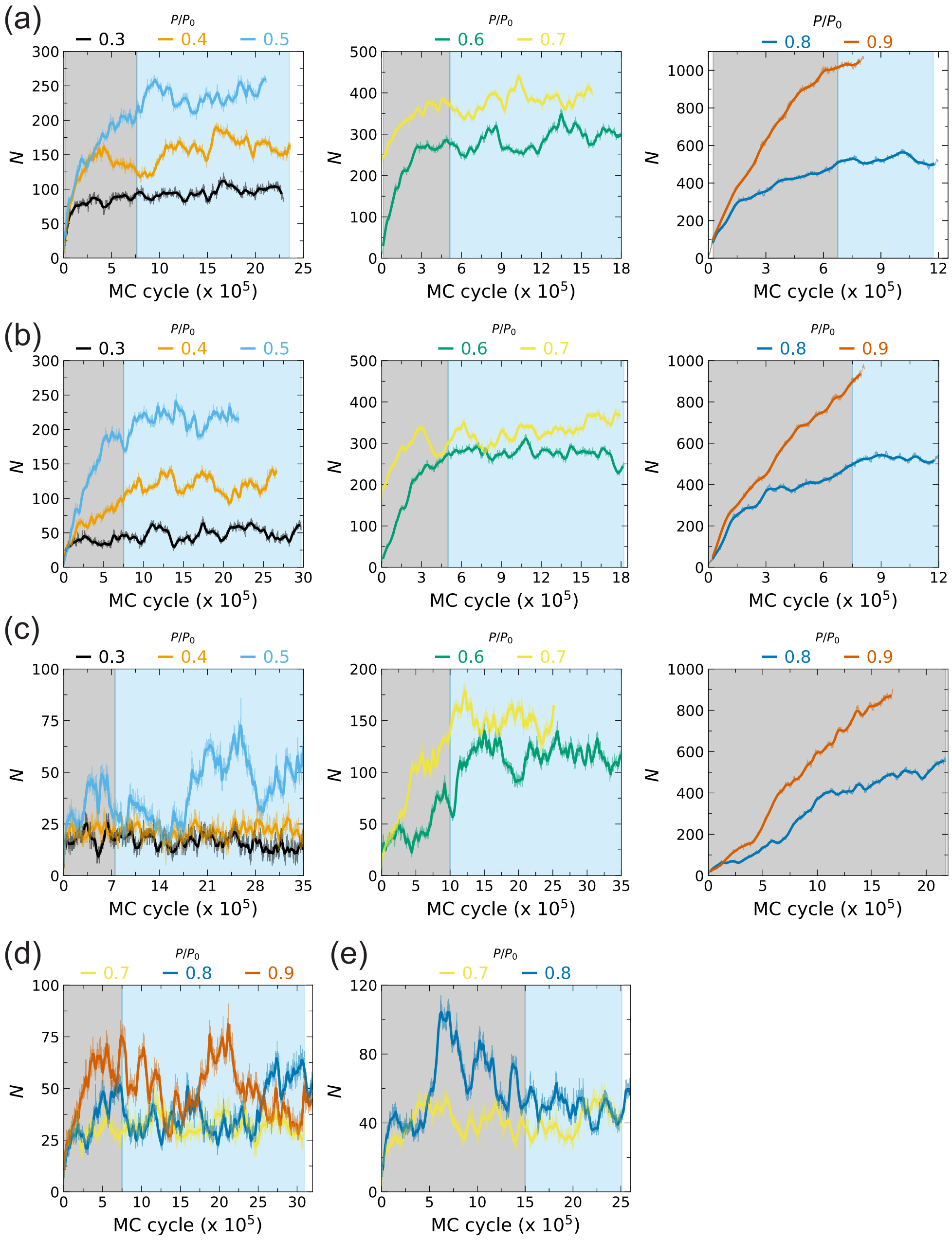

Fig. S5 Variation of number of water molecule adsorbed as a function of GCMC cycles for various relative pressures at T = 298 K for different GO surfaces with hydrophobic ratio of (a) H_R = 0, (b) H_R = 0.5, (c,d) H_R = 1, (e) H_R = 2, and (f) H_R = 3. Regions shaded with grey and light blue correspond to equilibration and production cycles, respectively. Data collected during the production cycle were used for the subsequent analysis. Note that in the case of H_R= 0 and 0.5, the system was not fully equilibrated for P/P$_0$ of 0.9, and for H_R= 1, the system was not fully equilibrated for relative P/P$_0$ of 0.8 and 0.9. At these relative pressures, the number of water molecules adsorbed in the system at the last GCMC cycle was taken for the adsorption isotherm.

Table S1 Ensemble averaged number of water molecules on both sides of GO surface for different hydrophobic ratio and relative pressures

H_R	P/P$_0$	$\langle N\rangle \pm \sigma_N$	$\sigma_N/\langle N\rangle(\%)$
0.0	0.2	66.53 ± 1.91	2.87
	0.3	95.51 ± 7.75	8.11
	0.4	157.49 ± 17.87	11.35
	0.5	235.02 ± 13.44	5.72
	0.6	287.5 ± 24.75	8.61
	0.7	381.22 ± 22.85	5.99
	0.8	523.74 ± 21.18	4.04
	0.9	1065	-
0.5	0.2	24.23 ± 3.5	14.44
	0.3	48.78 ± 9.23	18.92
	0.4	119.5 ± 11.87	9.93
	0.5	214.05 ± 14.14	6.61
	0.6	276.21 ± 14.56	5.27
	0.7	330.37 ± 23.02	6.97
	0.8	525.15 ± 14.92	2.84
	0.9	959	-
1.0	0.2	10.58 ± 3.52	33.27
	0.3	15.89 ± 3.82	24.04
	0.4	21.4 ± 3.92	18.32
	0.5	41.6 ± 14.3	34.375
	0.6	114.03 ± 14.83	13.0
	0.7	150.76 ± 11.09	7.36
	0.8	561	-
	0.9	897	-
2.0	0.7	32.0 ± 5.25	16.41
	0.8	38.29 ± 11.04	28.83
	0.9	49.69 ± 12.81	25.78
3.0	0.7	40.49 ± 8.25	20.375
	0.8	51.65 ± 8.46	16.38

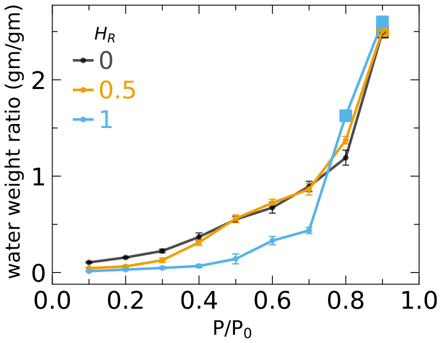

Fig. S6 Adsorption isotherms of water on GO surfaces as a function of relative pressure in terms of water weight ratio (gm of H_2O per gm of GO)

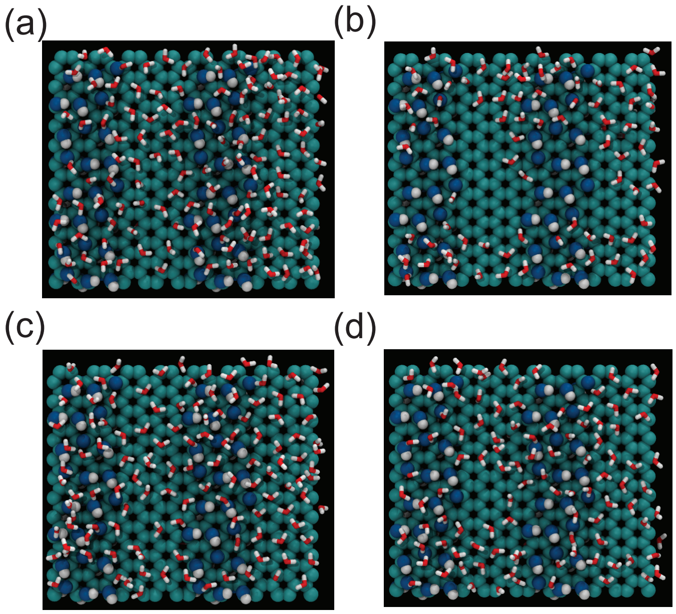

Fig. S7 Signature of the Janus surface in the GO surface of $H_R = 1$ at $P/P_0 = 0.6$. Representative snapshots of adsorbed water on the GO surface of $H_R = 1$ at $P/P_0 = 0.6$ and GCMC cycle (a) 15×10^5, (b) 20×10^5, (c) 22×10^5, and (d) 23×10^5. The GO surface and water molecules are represented in VdW sphere and licorice representation, respectively. Oxygen and hydrogen of H_2O, are shown in red, and white color, respectively. Carbon, oxygen and hydrogen atoms in the GO surface are shown in cyan, blue and white color, respectively.

Since we observed an asymmetric density distributions across the two surfaces on the GO surfaces, we checked the GCMC simulation procedure using a surface with top down symmetry. GCMC simulations were performed on a GO bilayer system ($H_R = 1$ surfaces) where both sides of surfaces that are exposed for water adsorption had a similar charge topology and a similar arrangement of functional groups as illustrated in Fig. S8a. The GCMC simulations for the relative pressure of 0.3, 0.5 and 0.6 were performed with 400000 MC cycles and last 200000 MC cycles with storing interval of 10 cycles were used for the density computations. Shown in Fig. S8a is the GO bilayer system where two GO surfaces of $H_R = 1$ are stacked with small interlayer spacing and both sides of GO surfaces have similar topology and charge. Figure S8b illustrates the density profiles of adsorbed water on this GO bilayer for relative pressures of 0.3, 0.5 and 0.6 at the temperature of 298 K. As expected, symmetric density profiles is seen on both sides of the GO surface validating our GCMC procedure. Thus we conclude that the observed density asymmetry (see Fig 2 in the main manuscript) is driven by the inherent and natural asymmetry present on the GO surfaces.

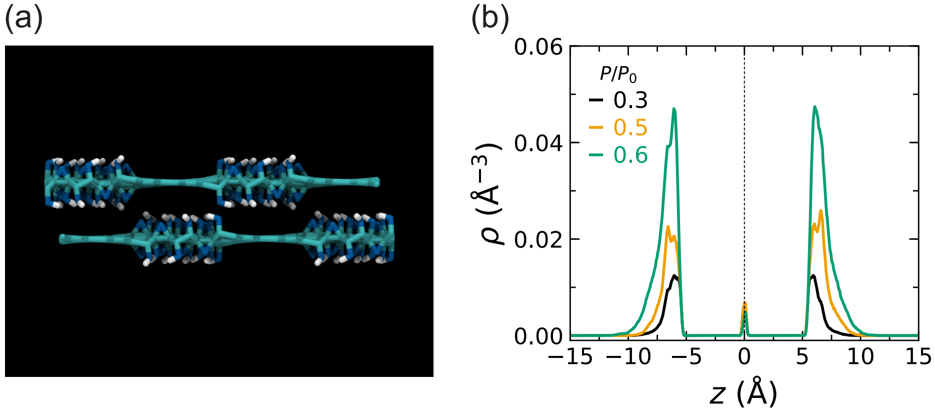

Fig. S8 (a) GO bilayer system which consists of two similar GO surfaces. The dimensions of GO surfaces are $L_x = 34.12$ Å and $L_y = 29.55$ Å. Carbon, oxygen and hydrogen atoms in the GO surface are shown in cyan, blue, and white colors, respectively. (b) Density distributions of water on GO bilayer system where both sides of GO bilayer surfaces are similar.

We have computed the average number of hydrogen bonds per water molecule according to the criteria mentioned in the main text. The hydrogen bonds for the hydroxyl group are higher than for the epoxy group for all relative pressures. As the relative pressure increases, the total number of hydrogen bonds increases, indicating that bulk-like behavior is approached.

Table S2 Average number of hydrogen bonds per water molecule for various relative pressures

P/P_0	N_{HB}^{epoxy}	$N_{HB}^{hydroxyl}$	N_{HB}^{Water}	N_{HB}^{total}
		$H_R = 0$		
0.1	0.54	1.582	0.341	2.463
0.2	0.457	1.41	0.748	2.615
0.3	0.381	1.164	1.18	2.725
0.4	0.258	0.808	1.842	2.908
0.5	0.198	0.633	2.19	3.021
0.6	0.178	0.517	2.37	3.065
0.7	0.126	0.367	2.66	3.153
0.8	0.093	0.281	2.82	3.194
0.9	0.047	0.147	3.06	3.254
		$H_R = 0.5$		
0.1	0.611	1.373	0.22	2.204
0.2	0.514	1.372	0.381	2.267
0.3	0.396	1.055	1.04	2.491
0.4	0.199	0.748	1.827	2.774
0.5	0.135	0.571	2.228	2.934
0.6	0.118	0.442	2.456	3.016
0.7	0.104	0.394	2.56	3.058
0.8	0.063	0.237	2.872	3.172
0.9	0.038	0.154	3.03	3.222
		$H_R = 1$		
0.1	0.423	0.684	0.315	1.422
0.2	0.365	0.607	0.635	1.607
0.3	0.307	0.567	0.915	1.789
0.4	0.33	0.538	0.983	1.851
0.5	0.276	0.482	1.386	2.144
0.6	0.148	0.29	2.328	2.766
0.7	0.122	0.254	2.492	2.868
0.8	0.057	0.143	2.906	3.106
0.9	0.036	0.088	3.067	3.191

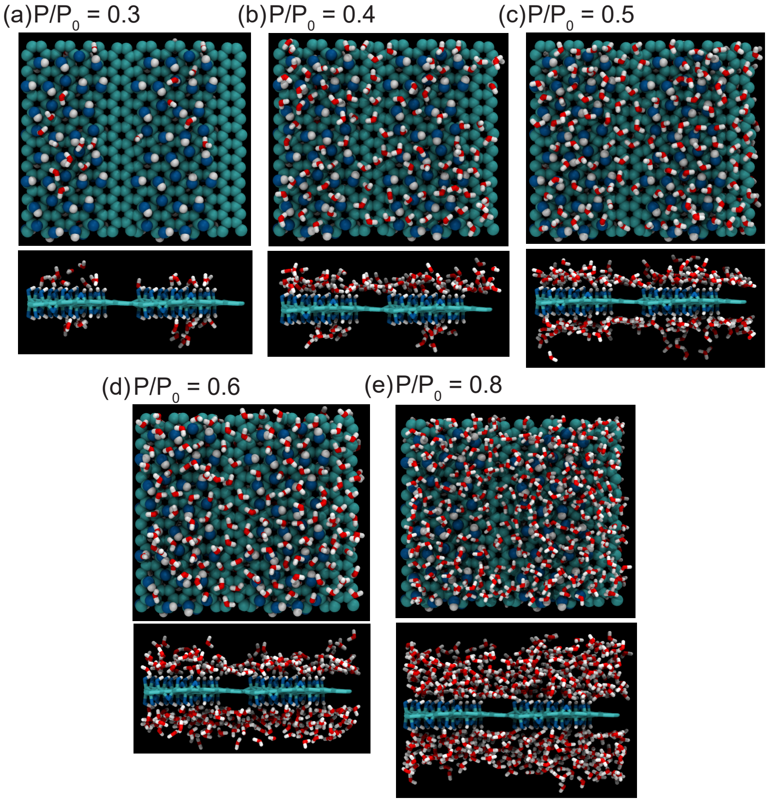

Fig. S9 Representative molecular snapshots of adsorbed water on the GO surface of H_R = 0.5 at the relative pressure of (a) $P/P_0 = 0.3$, (b) $P/P_0 = 0.4$, (c) $P/P_0 = 0.5$, (d) $P/P_0 = 0.6$, and (e) $P/P_0 = 0.8$. The GO surface and water molecules are represented in vdW sphere and licorice representations, respectively. Oxygen and hydrogen of H_2O, are shown in red, and white color, respectively. Carbon, oxygen and hydrogen atoms in the GO surface are shown in cyan, blue and white colors, respectively.

3 Molecular Dynamics Simulations

We have also computed the first rank of Legendre polynomial of the HH vector of interfacial water molecules. The orientational correlation function (C_1^{HH}) is evaluated using,

$$C_1^{\mathrm{HH}}(t) = \left\langle \frac{1}{N}\sum_{i=1}^{N} P_1(\mathbf{e}_i^{\mathrm{HH}}(t)\cdot\mathbf{e}_i^{\mathrm{HH}}(0)) \right\rangle, \tag{1}$$

where, $P_1(x) = x$ is the Legendre polynomial of rank 1, $\mathbf{e}^{\mathrm{HH}_i}$ is the unit vector of water molecule i along the HH axis in molecular frame. Angular brackets represent a shifted time average.

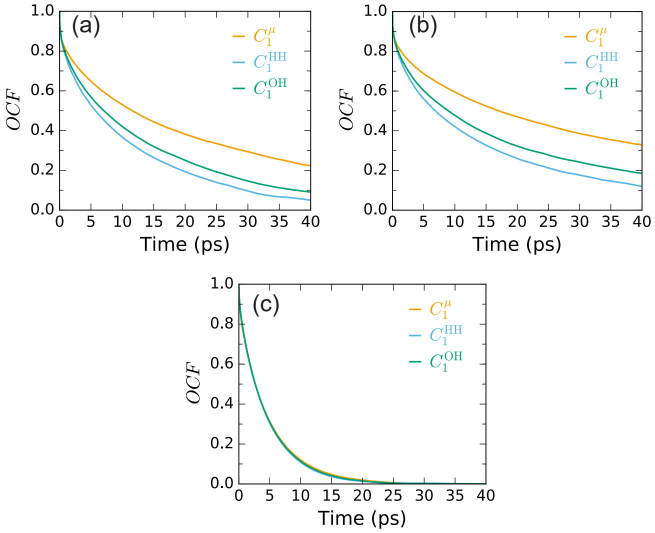

Fig. S10 Anisotropy in orientational relaxation Time evolution of dipole, OH, and HH vector correlation functions of interfacial water ($\rho_A = 0.125$ Å^{-2}) on (a) GO surface of $H_R = 1$ (b) GO surface of $H_R = 0$, and (c) bulk water at $T = 298$ K

We have fitted the C_1^{HH} function to a triple exponential function to obtain the relaxation time of the HH vector of interfacial water molecules. The parameters obtained from the fitting of the first rank Legendre polynomial of HH vector correlation function are given in Table S3. The values for bulk water are also reported for the comparison.

Table S3 Multi-exponential fitting parameters (see Eq. 4 in main manuscript) for the first rank HH vector, C_1^{HH} correlation functions for interfacial water molecules on the GO surfaces at 298 K. The relaxation time in the last column is evaluated using Eq. 5 in main manuscript.

GO Surface	ρ_A (Å^{-2})	a$_0$	τ_0 (ps)	a$_1$	τ_1 (ps)	a$_2$	τ_2 (ps)	$\tau_{l=1}^{\mathrm{HH}}$ (ps)
$H_R = 1$	0.05	0.1107	0.04805	0.0802	1.055	0.8091	24.57	22.449
	0.075	0.1011	0.04935	0.1275	1.161	0.7714	20.19	17.491
	0.1	0.1402	0.1722	0.1954	5.018	0.6644	19.2	15.9769
	0.125	0.1152	0.08605	0.1734	2.043	0.7114	15.16	12.5893
	0.15	0.1347	0.1623	0.2422	3.751	0.6231	15.09	11.9161
	0.2	0.1563	0.2953	0.5869	6.834	0.2568	20.4	10.9631
	0.3	0.1704	0.3784	0.7335	6.695	0.0961	31.87	9.6112
$H_R = 0$	0.05	0.134	0.05714	0.1982	3.151	0.6678	53.93	42.305
	0.075	0.1314	0.08481	0.1745	3.069	0.6941	27.02	22.21
	0.1	0.1463	0.1537	0.3372	5.812	0.5165	27.11	18.6975
	0.125	0.138	0.1341	0.2631	3.869	0.5989	24.38	18.11
	0.15	0.153	0.1887	0.2879	4.569	0.5591	15.44	11.7448
	0.2	0.1596	0.2629	0.4674	5.743	0.373	15.5	10.073
	0.3	0.1186	0.1308	0.4968	4.239	0.3846	13.9	8.4545
Bulk water	-	0.05918	0.01854	0.07212	0.558	0.8687	4.791	4.466

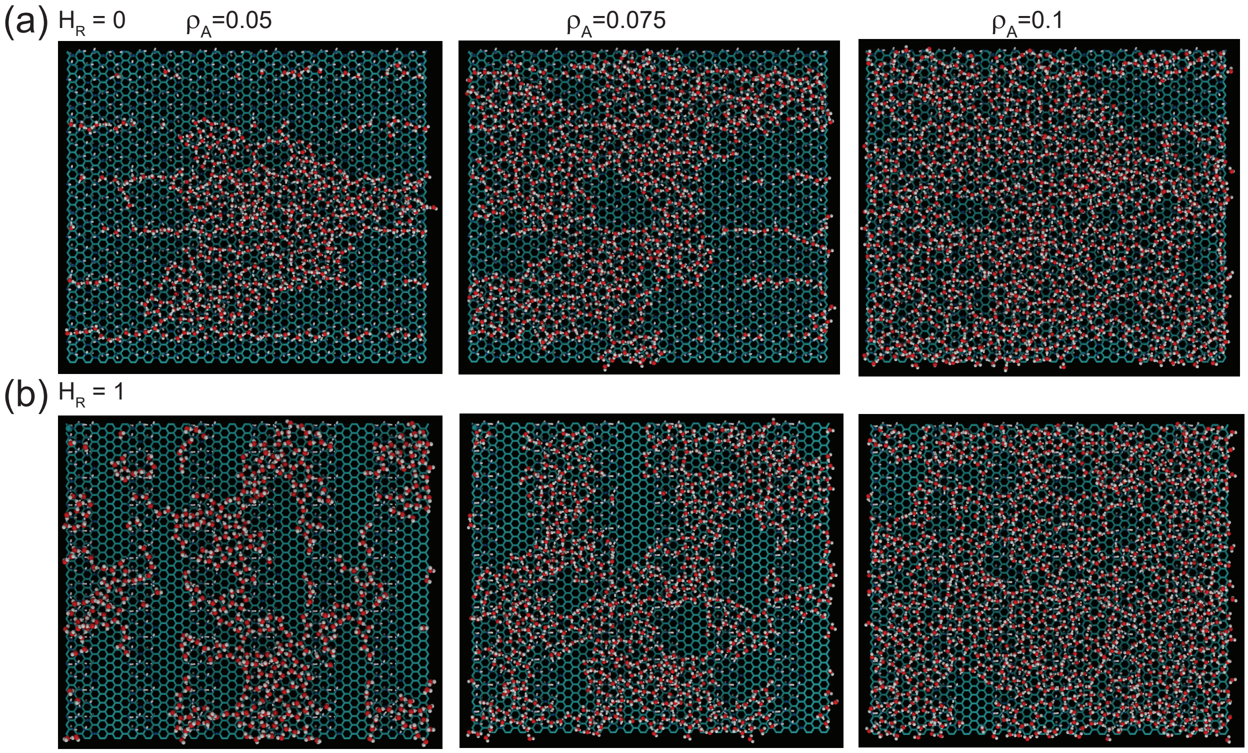

Fig. S11 Representative molecular snapshots of hydrogen bonds with water molecules on the GO surface of (a) $H_R = 0$ and (b) $H_R = 1$ for $\rho_A = 0.05$, 0.075 and 0.1. The GO surface and water molecules are represented in licorice and vdW sphere representations, respectively. Oxygen and hydrogen of H_2O, are shown in red, and white colors, respectively. Carbon, oxygen and hydrogen atoms in the GO surface are shown in cyan, blue and white colors, respectively.